AMERICAN SOCIETY FOR MICROBIOLOGY | Journal of Clinical Microbiology

Detection of Rare Drug Resistance Mutations by Digital PCR in a Human Influenza A Virus Model System and Clinical Samples

Alexandra S. Whale,[a] Claire A. Bushell,[a] Paul R. Grant,[b] Simon Cowen,[c] Ion Gutierrez-Aguirre,[d] Denise M. O'Sullivan,[a] Jana Žel,[d] Mojca Milavec,[d] Carole A. Foy,[a] Eleni Nastouli,[b] Jeremy A. Garson,[e] Jim F. Huggett[a,e]

Molecular and Cell Biology Team, LGC, Teddington, United Kingdom[a]; Virology Laboratory, Clinical Microbiology and Virology, University College London Hospital NHS Foundation Trust, London, United Kingdom[b]; Statistics Team, LGC, Teddington, United Kingdom[c]; National Institute of Biology, Ljubljana, Slovenia[d]; Department of Infection, Division of Infection and Immunity, University College London, London, United Kingdom[e]

Digital PCR (dPCR) is being increasingly used for the quantification of sequence variations, including single nucleotide polymorphisms (SNPs), due to its high accuracy and precision in comparison with techniques such as quantitative PCR (qPCR) and melt curve analysis. To develop and evaluate dPCR for SNP detection using DNA, RNA, and clinical samples, an influenza virus model of resistance to oseltamivir (Tamiflu) was used. First, this study was able to recognize and reduce off-target amplification in dPCR quantification, thereby enabling technical sensitivities down to 0.1% SNP abundance at a range of template concentrations, a 50-fold improvement on the qPCR assay used routinely in the clinic. Second, a method was developed for determining the false-positive rate (background) signal. Finally, comparison of dPCR with qPCR results on clinical samples demonstrated the potential impact dPCR could have on clinical research and patient management by earlier (trace) detection of rare drug-resistant sequence variants. Ultimately this could reduce the quantity of ineffective drugs taken and facilitate early switching to alternative medication when available. In the short term such methods could advance our understanding of microbial dynamics and therapeutic responses in a range of infectious diseases such as HIV, viral hepatitis, and tuberculosis. Furthermore, the findings presented here are directly relevant to other diagnostic areas, such as the detection of rare SNPs in malignancy, monitoring of graft rejection, and fetal screening.

In 2001 the World Health Organization (WHO) identified the threat of antimicrobial resistance as requiring immediate action with a need for worldwide cooperation (1). The development of new molecular methods for early diagnosis and monitoring of drug resistance is one such action (2, 3). In this study, digital PCR (dPCR) was employed to detect a clinically relevant single nucleotide polymorphism (SNP) in a human influenza A virus (H1N1) model involving resistance to the neuraminidase inhibitor oseltamivir (Tamiflu). Resistance is acquired by a *de novo* SNP mutation (p.H275Y) encoded in segment 6 of the viral genome (4) that changes the structure of the neuraminidase protein such that oseltamivir is unable to bind (5). This resistance conveys no loss of fitness to the virus, thus permitting transmission between humans and enabling resistance to spread (6). Between 1999 and 2002, oseltamivir resistance was present at a background rate of 0.33% in influenza A N1 virus isolates (4). However, since 2007 the spread of the resistant A (H1N1) virus has increased, and in 2008 the resistance rates were estimated to be up to 70% in some European countries (6). Subsequently, the WHO recommended vigilant monitoring for the emergence of oseltamivir resistance (7, 8). Since the disappearance of the 2009 pandemic A (H1N1) virus, the vast majority of circulating viruses are sensitive to oseltamivir (~99%) (9).

dPCR has been reported to enable detection of rare SNPs with technical sensitivities (also referred to as fractional abundance) down to 0.001% of the wild type (WT) in genomic DNA extracts (10, 11). To achieve this, dPCR subdivides a PCR into a large number of partitions so that a proportion of them contain no template molecules (12, 13). While this partitioning may increase the accuracy and precision of dPCR over the more widely used quantitative PCR (qPCR) (14–17), it may also improve the sensitivity when rare mutations are measured within a high-abundance WT background. Detection of rare SNPs by dPCR is being used in an increasing number of clinical applications, including cancer stratification (18, 19), fetal screening (20, 21), monitoring of organ transplant rejection (22), and detection of antimicrobial resistance (23, 24).

However, in order for such methods to be effectively applied in research and ultimately be translated into routine clinical analysis, validation of assay sensitivity is essential along with additional considerations such as cost, speed, and throughput. To achieve a given sensitivity, a PCR assay must first have sufficient specificity to allow confident discrimination between the SNP and WT molecules within a sample. Second, a very small number of mutant molecules must be detectable in the presence of a large excess of WT molecules.

Received 7 October 2015 **Returned for modification** 30 October 2015
Accepted 23 November 2015

Accepted manuscript posted online 9 December 2015

Citation Whale AS, Bushell CA, Grant PR, Cowen S, Gutierrez-Aguirre I, O'Sullivan DM, Žel J, Milavec M, Foy CA, Nastouli E, Garson JA, Huggett JF. 2016. Detection of rare drug resistance mutations by digital PCR in a human influenza A virus model system and clinical samples. J Clin Microbiol 54:392–400. doi:10.1128/JCM.02611-15.

Editor: A. J. McAdam

Address correspondence to Alexandra S. Whale, alexandra.whale@lgcgroup.com.

Supplemental material for this article may be found at http://dx.doi.org/10.1128/JCM.02611-15.

In this study, we addressed the issue of technical sensitivity, for which we evaluated the ability of dPCR to detect the p.H275Y SNP at abundances down to 0.1% of the WT in a range of nucleic acid concentrations using an *in vitro*-transcribed RNA material. We then validated our dPCR method by quantifying the p.H275Y SNP in clinical samples from patients who received oseltamivir treatment in comparison to a qPCR method that is used routinely in the clinic and that has an SNP detection sensitivity of 5%.

MATERIALS AND METHODS

Unless otherwise stated, experiments were performed in a single laboratory (LGC, United Kingdom), and all kits and instruments were used according to the manufacturers' instructions. RNA/DNA LoBind microcentrifuge tubes (Eppendorf) were used throughout the study.

Neuraminidase constructs and production of synthetic RNA transcripts. Segment 6 encompassing the full neuraminidase sequence for the human influenza A virus pandemic 2009 (H1N1) strain, containing either the sensitive wild-type sequence (WT, p.H275) or the oseltamivir drug resistance mutation (SNP. p.H275Y; C-to-T transition), was cloned into the pEX-K plasmid. To generate biologically relevant negative-strand RNA, *in vitro* transcription (IVT) of linearized plasmids was performed. IVT products were diluted to $\sim 1 \times 10^9$ copies/μl in carrier (15 ng/μl of RNA extracted from human lung cells [Ambion]) and stored in aliquots to reduce freeze-thawing effects. Full details are given in the supplemental material (see Section 1 and Fig. S1).

Clinical samples. Approval for use of clinical samples was given by UCLH Virology clinical governance in accordance with UCLH ethics guidance. Residual material originating from throat swabs (TS), nasal swabs (NS), combined throat and nasal swabs (CTNS), and endotracheal aspirates (ETA), as part of routine diagnostic laboratory practice in the Department of Clinical Microbiology and Virology at University College London Hospital (UCLH), were inactivated by mixing samples with an equal volume of buffer AL (Qiagen) prior to storage at 4°C for several weeks before they were transferred to −20°C for long-term storage. A positive (POS) SNP control was extracted from a cell culture (provided by R. Gunson, West of Scotland Specialist Virology Centre, Glasgow, Scotland) propagating a pandemic 2009 (H1N1) virus encoding the SNP. All viral RNA samples were extracted from 200 μl of clinical sample-buffer AL mix using an EZ1 Virus minikit, version 2.0, on a BioRobot EZ1 and eluted in 90 μl of AVE buffer (all Qiagen). These extracts were provided blind to LGC.

Design of the H275Y genotyping assay. A total of 733 pandemic (H1N1) virus neuraminidase gene sequences were downloaded from the NCBI influenza virus sequence database (25). These were aligned and viewed in the multiple-sequence alignment program Clustal X (26). The location of the oseltamivir drug resistance nucleotide mutation was identified. Primer Express, version 2.0, software (Applied Biosystems) was used to design two TaqMan minor groove binder (MGB) probes to the region containing the SNP, with one probe to target the wild-type (WT) sequence and the other to target the resistant (SNP) sequence. Universal primers were designed to flank the probe target sequence to generate a 74-bp amplicon (see Table S1 in the supplemental material).

Specificity to the pandemic (H1N1) virus serotype was determined by both *in silico* alignments (http://www.ncbi.nlm.nih.gov/genomes/FLU/FLU.html) and reverse transcription-qPCR (RT-qPCR). Prepandemic seasonal influenza A virus strains (H1N1 and H3N2), the avian influenza A virus (H5N1) strain, influenza B virus, and other common respiratory viruses (respiratory syncytial virus, parainfluenza viruses, human metapneumovirus, and adenovirus) were analyzed with the H275Y assay; none of these viruses were detected, demonstrating that the assay was specific to pandemic influenza A (H1N1) virus only. Details of the RT-qPCR method are given in the relevant section below and in the supplemental material (see Section 5).

Reverse transcription. All reverse transcription (RT) experiments were performed in accordance with the minimum information for publication of digital quantitative PCR experiments (dMIQE) guidelines (see Table S2 in the supplemental material) (27). The Maxima cDNA synthesis kit (Thermo Scientific) was used according to the manufacturer's instructions with the addition of 200 nM H275Y reverse primer to each 20-μl reaction mixture. For all experiments, triplicate RT reactions were performed with a single dPCR analysis per RT reaction. To monitor DNA contamination, reaction mixtures containing 1×10^5 IVT RNA copies per reaction volume with the reverse transcriptase omitted were performed; in all cases no amplification occurred (see Fig. S2F in the supplemental material). No-template controls (NTCs) were performed using carrier in place of template in every experiment; in all cases no DNA was detected (see Fig. S2A). RT was performed with an initial incubation at 25°C for 10 min, followed by RT at 50°C for 15 min. The enzyme was inactivated at 85°C for 5 min. The cDNA was either stored at −80°C or immediately analyzed by dPCR.

Digital PCR. dPCR experiments were implemented in accordance with the dMIQE guidelines (see Table S2 in the supplemental material) (27). dPCR experiments were performed using the QX100/QX200 Droplet Digital PCR (ddPCR) system (Bio-Rad). Reaction mixtures containing 1× ddPCR Supermix for probes with no dUTP (Bio-Rad), the H275Y assay (see Table S1 in the supplemental material; LGC_dPCR), and 2 μl of cDNA in a total volume of 20 μl were pipetted into the sample well of a DG8 cartridge. Droplet formation was performed as described previously (28). Thermocycling conditions were 95°C for 10 min, 40 cycles of 94°C for 30 s, and 60°C for 1 min, followed by 98°C for 10 min and a 4°C hold. The ramp rate for each step was set to 2°C/s. Droplets were read using a QX100/QX200 Droplet Reader, and the data were analyzed using QuantaSoft, version 1.6.6.0320. Thresholds were set to define the positive and negative droplets, and the data were exported as a comma-separated values (CSV) file. No-template controls (NTCs) were performed using water in place of template in every experiment; in all cases no amplification occurred (see Fig. S2A in the supplemental material). Optimization of the H275Y assay for dPCR was performed at two laboratories: LGC, United Kingdom, and NIB, Slovenia (see Section 2 in the supplemental material).

One-step reverse transcription-quantitative PCR. All RT-qPCR experiments were performed in accordance with the MIQE guidelines (see Table S3 in the supplemental material) (29). For H1N1 typing of the clinical samples at UCLH, a Superscript III Platinum One-Step qRT-PCR kit (Invitrogen) was used with an N1 typing assay published previously (Flu A H1N1 assay) (30). For the initial genotyping of the H275Y SNP in clinical samples at UCLH, a Superscript III Platinum One-Step qRT-PCR kit (Invitrogen) was used with the UCLH_H275Y assay. Comparison of RT-qPCR with dPCR results on the clinical samples at LGC was performed at LGC with an AgPath-ID One-Step RT-PCR Reagents kit (Applied Biosystems). Cycling and data capture were performed using a 7500 Fast or Prism 7900HT Real-Time PCR system (both Applied Biosystems). Analysis was performed using SDS software, version 2.4 (Applied Biosystems), to calculate the quantification cycle (C_q) values, and the data were exported as a CSV file. Full protocol conditions and experimental setups for all RT-qPCR methods are given in the supplemental material (see Section 5).

Data analysis. Exported CSV files from dPCR and qPCR experiments were imported into MS Excel 2010 or the R statistical programming environment (http://www.r-project.org/) for statistical analysis. For dPCR experiments, the average number of copies per partition (λ) with the associated confidence intervals were calculated in MS Excel 2010 as described previously (27, 31, 32). The mean values for template concentration and percent SNP [fractional abundance = $\lambda_{SNP}/(\lambda_{SNP} + \lambda_{WT})$] were calculated in MS Excel 2010 along with the associated standard deviation, coefficient of variance (CV), regression analysis (R^2), *t* tests, and analysis of variance (ANOVA). The RT efficiency was defined as the percent cDNA yield, calculated as $\lambda_{SNP}/\lambda_{exp}$, where λ_{exp} is the expected λ based on the concentration estimate using the Qubit 2.0 fluorimeter with a double-stranded DNA (dsDNA) high-sensitivity (HS) assay kit (Invitrogen). Where necessary, data were transformed by taking the natural logarithm

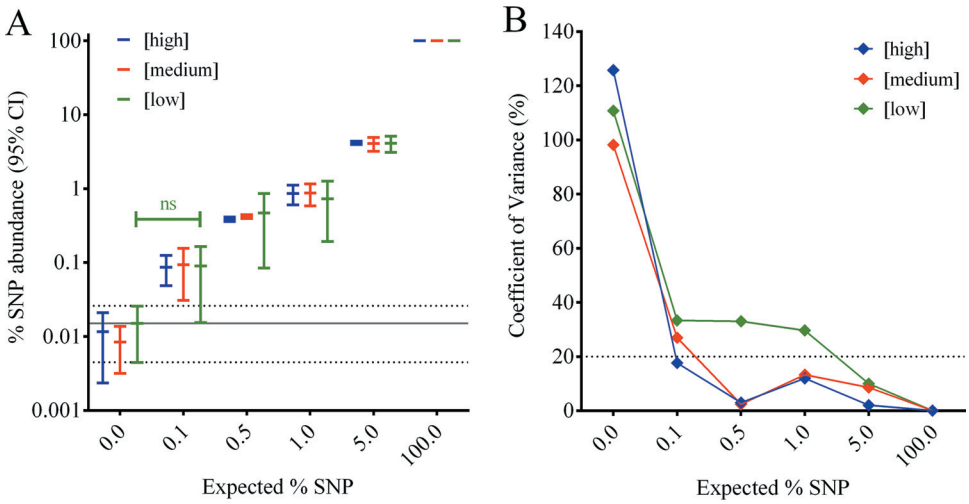

FIG 1 Measurement of mutant SNPs by digital PCR is dependent on template concentration and background signal. (A) Graph showing expected percent SNP of each sample (*x* axis) against the observed percent SNP abundance of the SNP molecule (*y* axis with log scale) for three concentrations, high, medium, and low. Each data point shows the mean and 95% confidence interval (CI) for the three experiments (performed on different days; 3 measurements), with the exception of the 0% SNP (WT-only) control that was performed in quadruplicate in all three experiments (12 measurements). The solid and dashed horizontal lines represent the mean and 95% confidence interval, respectively, of the low-concentration 0% SNP control. There was no significant (ns; $P > 0.05$) difference between the 0.1% and 0% SNP abundances for the low-concentration sample. All other SNP abundances and sample concentrations were significantly different ($P < 0.05$) from their respective 0% SNP controls. (B) Line graph showing the coefficients of variance (precision) of the measurements for the three sample concentrations. The horizontal dashed line indicates a CV of 20%.

(ln), as described previously (15). Figures were generated either directly from the software programs or using Prism, version 6 (GraphPad).

For the calculations of the false-positive rate (FPR), data were log transformed (λ and percent SNP) using the R statistical programming environment as described previously (15). A standard analytical chemistry method based on the dispersion of samples containing WT-only molecules was employed to compute the detection limits (33). The decision limits were calculated using two approaches: using the maximum observed value and an estimate based on Chebyshev's inequality (34). Full details are given in the supplemental material (see Section 4).

RESULTS

Evaluation of the sensitivity of digital PCR in quantification of rare single nucleotide polymorphisms. Initial experiments were performed to optimize and evaluate the ability of the QX100/200 dPCR system to detect the H275Y SNP using linearized plasmid DNA encoding either the WT or SNP sequence. The following parameters were investigated to optimize the specificity of the H275Y assay: primer and probe concentrations, MGB probe fluorophore dye swaps, uniplex and duplex reactions, and the annealing temperature (see Section 2 and Fig. S2 in the supplemental material). Duplex reaction mixtures containing 900 nM each primer and 250 nM each probe (SNP probe conjugated with 6-carboxyfluorescein [FAM] and a WT probe conjugated with VIC) with an annealing temperature of 60°C were selected for optimum specificity.

To evaluate the sensitivity of the method, a range of SNP abundances (between 100% and 0.1%) at different IVT RNA concentrations corresponding to different viral titers were generated: high concentration, 1.2×10^5 copies/RT reaction (expected cDNA λ of ~5.1, assuming 100% conversion rate of RNA to cDNA); medium concentration, 4×10^4 copies/RT reaction (λ of ~1.7); and low concentration, 2×10^4 copies/RT reaction (λ of ~0.85) (see Section 3 and Tables S4 and S5 in the supplemental material). The range of these viral loads represented those obtained from respiratory samples of patients with pandemic (H1N1) influenza A virus infection (35). The Maxima cDNA synthesis kit was selected due to the high conversion rate of RNA to cDNA (RT efficiency) obtained following reverse transcription (see Fig. S3). Each percent SNP at each concentration was measured with triplicate RTs (and one dPCR for each RT) in three independent experiments (9 data points per percent SNP at each concentration). For measurement of the false-positive rate (FPR) of the SNP assay (commonly referred to as the signal-to-noise ratio, or blank), WT-only (0% SNP) controls were also prepared at the three concentrations, with quadruplicate measurements made in each of the three experiments.

Strong linearity between the expected (as estimated by a Qubit 2.0 fluorimeter) and observed WT and SNP molecules per partition (λ) was measured for all experimental replicates (slope = 1.028, *y*-intercept = −0.076, $R^2 = 0.9962$) with no significant difference between the replicates ($P > 0.65$) (see Fig. S3A in the supplemental material). The RT efficiencies were normally distributed with averages of 88% (CV = 9%) and 76% (CV = 23%) for the WT and SNP assays, respectively (see Fig. S3B).

The smallest SNP abundance that could be measured as significantly different from that of the WT-only controls across all three RNA concentrations was 0.5% ($P < 0.036$). For both the high- and medium-concentration samples, the SNP molecule could also be resolved at 0.1% ($P < 0.024$ and $P < 0.013$, respectively) (Fig. 1A). The CV for each SNP abundance increased with reduced sample concentration; measurements of the high- and medium-concentration samples had a CV of <20% for SNP abundances of 100% to 0.5% while the 0.1% SNP had a CV of 17 and 21%, respectively. The low-concentration sample had a CV of >29% for all SNP abundances of 1% or less (Fig. 1B).

Defining the detection capability of dPCR. The detection of SNP molecules in the 0% SNP controls represents the FPR of the SNP assay and ranged from 0.06 to < 0.001% (average, 0.012%)

TABLE 1 Calculation of the detection capability[a]

Method	Sample concn	dPCR input (copies/rxn)[b]	Decision limit (ln λ)	Detection capability		
				ln λ	ln % SNP abundance	% SNP abundance
Maximum observed value	High	120,000	−6.349	−5.965	−7.54	0.05
	Medium	40,000	−8.078	−7.694	−8.11	0.03
	Low	20,000	−7.645	−7.261	−6.96	0.10
Chebyshev's inequality ($\alpha = 0.05$)	High	120,000	−5.784	−5.400	−6.96	0.09
	Medium	40,000	−7.505	−7.121	−7.53	0.05
	Low	20,000	−7.300	−6.916	−6.61	0.13

[a] For full details for calculation of these values, see the text and supplemental material.
[b] rxn, reaction.

across the three different sample concentrations (Fig. 1A). The observed variance associated with these controls was heteroscedastic with a CV of >90% (Fig. 1B). The limit of detection (LOD) of an assay is linked to the FPR and its associated variance: the lower the FPR, the smaller the abundance of the SNP that can be measured as significantly different from that of the WT-only control. Therefore, it was hypothesized that the theoretical limit of detection for a given sample concentration could be extrapolated from the experimental FPR data.

Using two methods, the maximum observed value and Chebyshev's inequality (34), the decision limit and the detection capability were calculated (Table 1; see also Fig. S4 in the supplemental material). The detection capability, which defines the LOD in this context, was lower than the values tested experimentally for the high- and medium-concentration samples (Table 1). Chebyshev's inequality, which generates more conservative estimates, defined the limit of detection as 0.13% for the low-concentration sample (Table 1) and is consistent with the inability to detect the 0.1% SNP abundance in the low-concentration sample as significantly different from that of the WT-only controls.

Identification of oseltamivir resistance mutants in patients with influenza A H1N1 virus infection. Following the 2009 influenza A virus H1N1 pandemic, the H1N1 type was detected in patients undergoing oseltamivir treatment at UCLH with the one-step RT-qPCR method using the Flu A H1N1 assay (30). Patient samples were screened for oseltamivir resistance using a one-step RT-qPCR method (UCLH_RT-qPCR) to identify the presence of WT (oseltamivir-sensitive) and/or SNP (oseltamivir-resistant) molecules (Table 2 and Fig. 2).

Absolute quantification of the clinical samples by RT-qPCR was performed using standard curves generated from the IVT RNA (LGC_RT-qPCR). The limit of detection was defined as 75

TABLE 2 Analysis of clinical samples by qPCR and dPCR

Patient code or control	Day	Sample type[a]	Flu A H1N1 assay result[b]	UCLH_RT-qPCR result[c]	LGC_RT-qPCR		LGC_dPCR	
					Total viral load (log_{10} copies/ml of extract)	Result[c]	Total viral load (log_{10} copies/ml of extract)	Result[c]
P1.1	0	TS	+	**Sen**	**4.35**	**FP**	**3.92**	**Sen**
P1.2	26	TS	ND	ND		ND		ND
P1.3	28	CTNS	+	**Res**	**5.34**	**Res**	**4.53**	**Res**
P1.4	29	CTNS	+	**Res**	**5.54**	**Res**	**4.96**	**Res**
P1.5	32	TS	LLP	Res		ND		ND
P2	0	TS	+	Res		ND		ND
P3.1	0	CTNS	+	**Sen**	**3.49**	**Sen**	**3.51**	**Sen**
P3.2	5	CTNS	+	Res		ND	3.78	Sen
P3.3	11	NS	ND	ND		ND	3.36	Sen
P3.4	15	CTNS	ND	ND		ND	3.51	Sen
P4.1	0	ETA	+	ND	4.59	Sen		ND
P4.2	0	CTNS	ND	ND		ND	3.04	Sen
P4.3	5	CTNS	ND	ND		ND		ND
P5.1	0	ETA	+	**Sen**	**5.48**	**FP**	**4.56**	**Sen**
P5.2	12	CTNS	ND	ND		ND	3.69	Sen
P6	0	CTNS	LLP	ND		ND		ND
P7	0	CTNS	LLP	ND		ND		ND
P8	0	TS	+	**Sen**		ND	**3.03**	**Sen**
POS			+	**Res**	**3.23**	**Res**	**3.61**	**Res**
NEG			ND	**ND**		**ND**		**ND**

[a] TS, throat swab; NS, nasal swab; CTNS, combined throat and nasal swab; ETA, endotracheal aspirate.
[b] +, positive by PCR; ND, not detected/below the limit of detection; LLP, low-level positive.
[c] Res, resistant sequences (SNP) detected in sample; Sen, only sensitive sequences (WT) detected; FP, false positive (see text for details). Boldface, concordance between LGC and UCLH results; underlining, sample identified as positive for H1N1 by UCLH_RT-qPCR with the detection of both WT and SNP sequences.

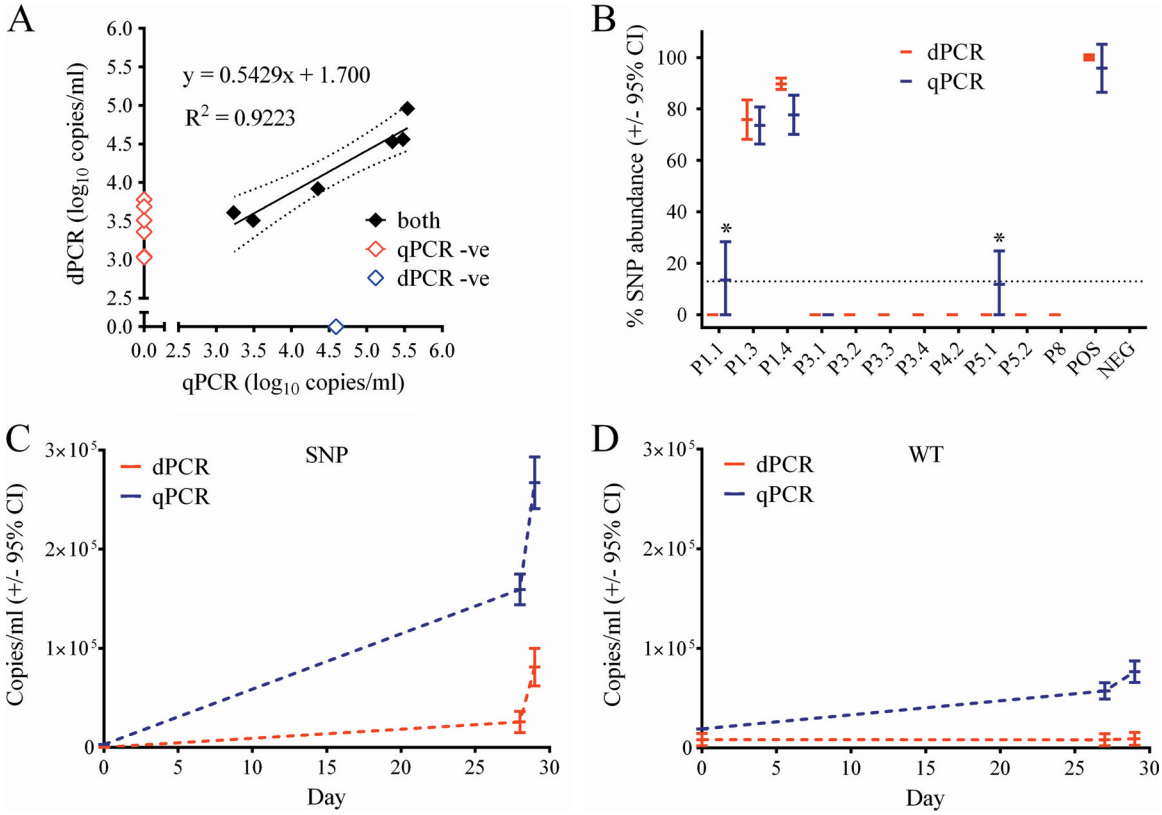

FIG 2 Identification of oseltamivir-resistant mutants in patients with influenza A H1N1 virus infection. (A) Linear regression for the 18 clinical samples. Data are plotted as the $\log_{10}$ total RNA copies (WT and SNP) per milliliter of clinical sample extract between two-step dPCR and one-step RT-qPCR. The regression line (solid line) with its associated 95% confidence interval (CI; dashed lines) is shown. (B) Percent SNP abundance measured in each clinical sample (*x* axis) by two-step LGC_dPCR (red) and one-step LGC_RT-qPCR (blue). A single mean value (horizontal dash in red or blue) at 0% indicates a sample in which only WT sequences were measured. Error bars represent the 95% confidence interval in the measurement of the percent SNP. The solid and dashed horizontal lines represent the limits of detection of the SNP assay by LGC_RT-qPCR. Two samples were identified as false positives (*). (C and D) Longitudinal quantification of SNP and WT sequences in patient 1 over 1 month by dPCR and qPCR. POS, SNP-only positive control; NEG, negative control (extraction buffer only).

RNA copies/reaction product (equivalent viral load of 2.65 $\log_{10}$ copies/ml of extract) (see Fig. S6B in the supplemental material) with a specificity for the WT and SNP probes of 90% and 87%, respectively, regardless of sample concentration (see Fig. S6C). Due to the number of samples that were quantified by dPCR only, comparison of LGC_RT-qPCR and dPCR measurements identified a poor linear correlation. Analysis of the six samples that were quantified by both dPCR and LGC_RT-qPCR identified a good linear correlation (R^2 = 0.9223). The gradient of the slope (0.5429) was significantly different from 1 ($P = 0.04$), indicating a measurement bias (Fig. 2A). The CV was on average lower for the dPCR measurements than for qPCR (13% and 23%, respectively). Spike-in experiments confirmed the absence of inhibitors carried over from the sampling or extraction process disrupting the qPCRs or dPCRs (see Fig. S6D).

Fairly good concordance for detection of WT and SNP molecules was observed between the UCLH_RT-qPCR, LGC_RT-qPCR, and dPCR results (Table 2, boldface values). Five samples had very low concentrations as defined by dPCR (samples 3.2, 3.3, 3.4, 4.2, and 5.2) and were below the limit of sensitivity for qPCR. Furthermore, only one of these five clinical samples was identified as positive for H1N1 by UCLH_RT-qPCR (sample 3.2) with the detection of both WT and SNP sequences (Table 2, underlined values). WT sequences were detected in one sample (sample 4.1) by LGC_RT-qPCR at LGC while no sequences were detected by UCLH_RT-qPCR or by dPCR.

Both WT and SNP molecules were identified in two clinical samples by LGC_RT-qPCR and dPCR (samples P1.3 and P1.4) (Fig. 2B). SNP molecules were measured in a further two clinical samples by LGC_RT-qPCR but not by dPCR (Fig. 2B); the proportions of SNP molecules as measured by LGC_RT-qPCR were 13.53% and 11.86% for samples 1.1 and 5.1, respectively (Fig. 2B, asterisks). As the limit of specificity of the assay was defined as 87%, these samples were identified as potential false positives for the presence of the SNP molecule as the uncertainty in their quantification was above the limit of the specificity for the SNP assay (Table 2). Absence of amplification of either molecule in the experimental negative controls (NEG) indicated that the SNP signal was unlikely to be caused by contaminating molecules (Fig. 2B). The limitations of the specificity of the LGC_RT-qPCR assay were further highlighted in the analysis of the SNP-only sample (POS), where the SNP abundance was measured as 95.82% (Fig. 2B).

Five samples were taken from patient 1 over the course of a month during treatment with oseltamivir (samples 1.1 to 1.5). Longitudinal analysis of the concentration of the WT and SNP molecules revealed that the SNP molecule became predomi-

nant by day 28. From days 28 to 29, the amount of SNP molecules quantified by both qPCR and dPCR increased nearly 2-fold (Fig. 2C). While the concentration of the WT molecule stayed constant over the duration as measured by dPCR, it significantly increased over 1.5-fold ($P = 0.003$) when measured by qPCR (Fig. 2D).

DISCUSSION

Using a human influenza A virus model system, we have developed a dPCR method for rare drug resistance mutations. We have investigated a number of challenges associated with SNP detection, namely, the specificity, sensitivity, and the false-positive rate (FPR) of an assay. We then validated our method using clinical samples.

Our study has confirmed the ability to recognize and reduce off-target amplification (mismatch binding of WT probe with the SNP sequence and vice versa), thereby improving the specificity of the assay and so tackling one of the great challenges of SNP detection. We have demonstrated the ability of dPCR to detect rare SNPs down to 0.1% abundance (Fig. 1) although it should be acknowledged that this was using material generated from IVTs in a background of human lung RNA and so does not take into account the effects more complex respiratory matrices may have on the reaction.

While there is currently no clinical data demonstrating the necessity of detecting SNPs down to 0.1% abundance, by developing a method with increased levels of sensitivity, we provide the means by which future studies could determine an appropriate cutoff for clinical use and by which the development of resistance can be more accurately monitored during treatment. Indeed, there is a need to consistently measure the 1% population abundance that is the current background rate of the mutation (4, 6, 9) in order to follow the recommended WHO guidelines (7, 8). The same assay (primers and probes) in qPCR has a cutoff at approximately 5% abundance due to the off-target amplification of the WT molecules with the SNP probe (36), and therefore our study represents a 50-fold increase in sensitivity by dPCR. This is consistent with the reported limits of other qPCR assays for SNP detection (37, 38) and with the identification of false-positive results for two clinical samples (P1.1 and P5.1) that were identified as containing SNP sequences by qPCR only.

The increased sensitivity of dPCR over qPCR was shown by the proportion of clinical samples that were detectable by dPCR only (Fig. 2A and B). A recent study using a different assay that targets the same H275Y SNP observed comparable differences in the sensitivities between qPCR and dPCR (24). While improved quantification and precision of dPCR over qPCR have also been observed in other RNA viral models (39, 40), studies using infectious agents with DNA genomes have shown further improvement in the quantification and precision by both dPCR and qPCR (41, 42). This suggests that the RT step could have a greater effect on the sensitivity of qPCR although dPCR is not immune from variability in the RT efficiency (see Fig. S3B in the supplemental material). However, it is acknowledged that without a third method to arbitrate the discrepancies between qPCR and dPCR results, we cannot be certain that the dPCR result is the correct result.

In addition to the off-target amplification, the greater specificity and sensitivity afforded by dPCR, with respect to qPCR, are related to both the FPR and precision of the measurement. Here, we developed a method to define the FPR that is associated with the sample concentration. When sample concentration is not limiting and a DNA template is used, it is possible to detect abundances down to 0.001% using dPCR, as demonstrated in two genomic DNA cancer models (10, 11). While this is impressive, there are a number of other factors that prevent sensitivities of this magnitude from being routinely achieved in clinical samples.

The sample concentration limits are self-explanatory; to detect 0.001% sequence abundance, substantially more than 100,000 sequences must be measured (equates to a viral titer of >8 $\log_{10}$ copies/ml). However, a sample is influenced not only by the sample concentration but also by the quality of the sample; for example, sputum-containing samples can be difficult to homogenize prior to extraction (43, 44). The type of respiratory samples used in this study involved RNA extracted from TS, NS, CTNS, and endotracheal aspirate (ETA), which could also have an impact on the results and may be a contributing factor to the difference in performance between qPCR and dPCR. It has previously been shown that inhibitors carried over from the extraction process in a cytomegalovirus (CMV) model affect qPCR and dPCR to different extents (45). Furthermore, the RNA yield obtained from extraction of RNA from influenza viruses from sputum can vary from 20 to 100%, depending on the extraction method used (43). These are important areas for future investigation into the ability of dPCR to measure rare sequences in RNA viruses.

Additional considerations include the sample concentration; as this is reduced, the associated precision of dPCR is also reduced, although not to the same extent as with qPCR, and so smaller differences between samples could be harder to measure with confidence (46). While these factors may have implications for clinical samples such as those used in this study, it is also of importance for the longitudinal monitoring of patients whose viral loads are expected to decrease in response to treatment over time.

This is clearly demonstrated by the analysis of longitudinal samples from a single patient (Fig. 2C and D); dPCR measured the WT molecules as remaining at a constant level while there was an increase in the abundance of the SNP molecule during treatment. In contrast, LGC_RT-qPCR measured an increase in both the WT and SNP molecules and so implied that, despite treatment, the overall viral load of the patient was increasing. Recently, a similar longitudinal analysis of a patient infected with oseltamivir-resistant H1N1 influenza A virus demonstrated that dPCR is less prone to operator effects than qPCR and has reduced interassay and intra-assay variability in SNP quantification (24). Together, these findings show the potential advantages of dPCR for monitoring and surveillance of antimicrobial drug resistance.

In this study, we demonstrated that the FPR determined the technical sensitivity of the low-concentration sample rather than the precision of dPCR, which therefore demonstrates that the FPR is linked with the sample concentration. A separate study investigating SNP mutations in a cfDNA model identified the FPR as being independent of sample concentration (18); however, this study was investigating the genotype of cell-free DNA (cfDNA) extracted from plasma, and so the WT sequences were very low in concentration, indicating that the FPR can be difficult to define in very low concentration samples. The FPR of an assay can be split into two sources, experimental and technical. Experimental FPR can be attributed to laboratory contamination that was absent in this study (see Fig. S2 and Table S5 in the supplemental material)

and is reduced by appropriate optimization and good laboratory practice.

This leaves the technical sources contributing to the FPR that are harder to define but could include off-target amplification and enzymatic errors, such as those that arise from reverse transcriptases and/or polymerases (47). By defining the limit of detection mathematically and relating it to the concentration of the sample as described, experimental constraints that limit the number of negative controls (for example, different dPCR platforms have different maximum sample numbers per experiment) could be overcome (46). This is in sharp contrast to other methods, such as qPCR, which is limited by the quality of the calibration curve, or next-generation sequencing, which can be limited by technical error rates (48).

Finally, the robustness of dPCR allowed a qPCR assay that is used routinely in the clinic to be transferred onto a dPCR platform with minimal optimization. Furthermore, the reproducibility of dPCR compared with that of qPCR (24) demonstrates the potential of dPCR for clinical use. Various other methods such as competitive allele-specific TaqMan (CAST) PCR (38, 49, 50), an amplification-refractory mutation system (ARMS) (51), and the use of locked nucleic acid (LNA) probes (52, 53) have been developed to improve the 5 to 10% SNP abundance limit of qPCR. While these methods are capable of detecting down to 0.1 to 1% SNP, they require extensive optimization, including in some cases a total redesign of the assay.

Despite all of these advantages, in the short term the nonreliance of dPCR on calibration materials for quantification could be exploited as an alternative value assignment method that is independent of mass or fluorescent measurements (54). Previous studies have shown that UV spectrometry methods can overquantify nucleic acid abundance compared with results from dPCR (14, 16). Therefore, the apparently higher concentrations of the clinical samples as measured by qPCR than by dPCR (Fig. 2A) could be attributed to the inherent limitations of the UV quantification of the IVT RNA used for the calibration curve rather than to bias within the qPCR method itself.

The ability of dPCR to detect rare drug resistance SNP mutations could enable earlier detection, facilitating earlier switching to alternative therapeutic agents and resulting in an overall reduction in the amount of ineffective drugs used. This should result in a reduction in both drug resistance and cost. Other infectious diseases such as HIV, viral hepatitis, and bacterial infections including tuberculosis and gonorrhea could also benefit from this approach to antimicrobial drug resistance monitoring. Finally, the findings of this study should be applicable in a wide range of other diagnostic areas, including the monitoring of cell-free nucleic acid in malignancy and fetal screening.

ACKNOWLEDGMENTS

We acknowledge George Karlin-Neumann and Svilen Tzonev from Bio-Rad for extensive assistance in the development of this study and Rory Gunson of the West of Scotland Specialist Virology Centre in Glasgow, who kindly donated the cell culture propagating a pandemic H1N1 virus encoding the H275Y mutation.

The work described in the manuscript was partially funded by the United Kingdom National Measurement System (NMS) and the European Metrology Research Programme (EMRP) joint research project (HLT08) Infect-Met (http://infectmet.lgcgroup.com) which is jointly funded by the EMRP participating countries within EURAMET and the European Union.

FUNDING INFORMATION

UK National Measurement System provided funding to Alexandra S. Whale, Clarie Bushell, Simon Cowen, Denise M. O'Sullivan, Carole A. Foy, and Jim F. Huggett. European Metrology Research Programme (EMRP) provided funding to Alexandra S. Whale, Clarie Bushell, Simon Cowen, Ion Gutierrez-Aguire, Denise M. O'Sullivan, Jana Žel, Mojca Milavec, Carole A. Foy, and Jim F. Huggett under grant number HLT08.

REFERENCES

1. **WHO.** 2001. WHO global strategy for containment of antimicrobial resistance. World Health Organization, Geneva, Switzerland. http://www.who.int/entity/csr/resources/publications/drugresist/en/EGlobal_Strat.pdf.
2. **van der Vries E, Anber J, van der Linden A, Wu Y, Maaskant J, Stadhouders R, van Beek R, Rimmelzwaan G, Osterhaus A, Boucher C, Schutten M.** 2013. Molecular assays for quantitative and qualitative detection of influenza virus and oseltamivir resistance mutations. J Mol Diagn **15:**347–354. http://dx.doi.org/10.1016/j.jmoldx.2012.11.007.
3. **van der Vries E, Schutten M, Fraaij P, Boucher C, Osterhaus A.** 2013. Influenza virus resistance to antiviral therapy. Adv Pharmacol **67:**217–246. http://dx.doi.org/10.1016/B978-0-12-405880-4.00006-8.
4. **Monto AS, McKimm-Breschkin JL, Macken C, Hampson AW, Hay A, Klimov A, Tashiro M, Webster RG, Aymard M, Hayden FG, Zambon M.** 2006. Detection of influenza viruses resistant to neuraminidase inhibitors in global surveillance during the first 3 years of their use. Antimicrob Agents Chemother **50:**2395–2402. http://dx.doi.org/10.1128/AAC.01339-05.
5. **Moscona A.** 2005. Oseltamivir resistance: disabling our influenza defenses. N Engl J Med **353:**2633–2636. http://dx.doi.org/10.1056/NEJMp058291.
6. **Lackenby A, Hungnes O, Dudman SG, Meijer A, Paget WJ, Hay AJ, Zambon MC.** 2008. Emergence of resistance to oseltamivir among influenza A(H1N1) viruses in Europe. Euro Surveill **13:**8026. http://www.eurosurveillance.org/ViewArticle.aspx?ArticleId=8026.
7. **WHO.** 2009. Oseltamivir resistance in immunocompromised hospital patients; pandemic (H1N1) 2009 briefing note 18. World Health Organization, Geneva, Switzerland. http://www.who.int/csr/disease/swineflu/notes/briefing_20091202/en/index.html.
8. **WHO.** 2009. Viruses resistant to oseltamivir (Tamiflu) identified; pandemic (H1N1) 2009 briefing note 1. World Health Organization, Geneva, Switzerland. http://www.who.int/csr/disease/swineflu/notes/h1n1_antiviral_resistance_20090708/en/index.html.
9. **Meijer AJM, van Beek P, Swaan CM, Osterhaus AD, Daniels RS, Hurt AC, Koopmans MP.** 2012. Oseltamivir-resistant influenza A(H1N1)pdm09 virus in Dutch travellers returning from Spain. Euro Surveill **17:**20266. http://www.eurosurveillance.org/ViewArticle.aspx?ArticleId=20266.
10. **Pekin D, Skhiri Y, Baret JC, Le Corre D, Mazutis L, Salem CB, Millot F, El Harrak A, Hutchison JB, Larson JW, Link DR, Laurent-Puig P, Griffiths AD, Taly V.** 2011. Quantitative and sensitive detection of rare mutations using droplet-based microfluidics. Lab Chip **11:**2156–2166. http://dx.doi.org/10.1039/c1lc20128j.
11. **Hindson BJ, Ness KD, Masquelier DA, Belgrader P, Heredia NJ, Makarewicz AJ, Bright IJ, Lucero MY, Hiddessen AL, Legler TC, Kitano TK, Hodel MR, Petersen JF, Wyatt PW, Steenblock ER, Shah PH, Bousse LJ, Troup CB, Mellen JC, Wittmann DK, Erndt NG, Cauley TH, Koehler RT, So AP, Dube S, Rose KA, Montesclaros L, Wang S, Stumbo DP, Hodges SP, Romine S, Milanvich FP, White HE, Regan JF, Karlin-Neumann GA, Hindson CM, Saxonov S, Colston BW.** 2011. High-throughput droplet digital PCR system for absolute quantitation of DNA copy number. Anal Chem **83:**8604–8610. http://dx.doi.org/10.1021/ac202028g.
12. **Sykes PJ, Neoh SH, Brisco MJ, Hughes E, Condon J, Morley AA.** 1992. Quantitation of targets for PCR by use of limiting dilution. Biotechniques **13:**444–449.
13. **Vogelstein B, Kinzler KW.** 1999. Digital PCR. Proc Natl Acad Sci U S A **96:**9236–9241. http://dx.doi.org/10.1073/pnas.96.16.9236.
14. **Sanders R, Huggett JF, Bushell CA, Cowen S, Scott DJ, Foy CA.** 2011. Evaluation of digital PCR for absolute DNA quantification. Anal Chem **83:**6474–6484. http://dx.doi.org/10.1021/ac103230c.
15. **Whale AS, Huggett JF, Cowen S, Speirs V, Shaw J, Ellison S, Foy CA, Scott DJ.** 2012. Comparison of microfluidic digital PCR and conventional

quantitative PCR for measuring copy number variation. Nucleic Acids Res **40:**e82. http://dx.doi.org/10.1093/nar/gks203.
16. **Sanders R, Mason DJ, Foy CA, Huggett JF.** 2013. Evaluation of digital PCR for absolute RNA quantification. PLoS One **8:**e75296. http://dx.doi.org/10.1371/journal.pone.0075296.
17. **Hindson CM, Chevillet JR, Briggs HA, Gallichotte EN, Ruf IK, Hindson BJ, Vessella RL, Tewari M.** 2013. Absolute quantification by droplet digital PCR versus analog real-time PCR. Nat Methods **10:**1003–1005. http://dx.doi.org/10.1038/nmeth.2633.
18. **Taly V, Pekin D, Benhaim L, Kotsopoulos SK, Le Corre D, Li X, Atochin I, Link DR, Griffiths AD, Pallier K, Blons H, Bouche O, Landi B, Hutchison JB, Laurent-Puig P.** 2013. Multiplex picodroplet digital PCR to detect KRAS mutations in circulating DNA from the plasma of colorectal cancer patients. Clin Chem **59:**1722–1731. http://dx.doi.org/10.1373/clinchem.2013.206359.
19. **Laurent-Puig P, Pekin D, Normand C, Kotsopoulos SK, Nizard P, Perez-Toralla K, Rowell R, Olson J, Srinivasan P, Le Corre D, Hor T, El Harrak Z, Li X, Link DR, Bouche O, Emile JF, Landi B, Boige V, Hutchison JB, Taly V.** 2015. Clinical relevance of KRAS-mutated subclones detected with picodroplet digital PCR in advanced colorectal cancer treated with anti-EGFR therapy. Clin Cancer Res **21:**1087–1097. http://dx.doi.org/10.1158/1078-0432.CCR-14-0983.
20. **Barrett AN, McDonnell TC, Chan KC, Chitty LS.** 2012. Digital PCR analysis of maternal plasma for noninvasive detection of sickle cell anemia. Clin Chem **58:**1026–1032. http://dx.doi.org/10.1373/clinchem.2011.178939.
21. **Lench N, Barrett A, Fielding S, McKay F, Hill M, Jenkins L, White H, Chitty LS.** 2013. The clinical implementation of non-invasive prenatal diagnosis for single-gene disorders: challenges and progress made. Prenat Diagn **33:**555–562. http://dx.doi.org/10.1002/pd.4124.
22. **Beck J, Bierau S, Balzer S, Andag R, Kanzow P, Schmitz J, Gaedcke J, Moerer O, Slotta JE, Walson P, Kollmar O, Oellerich M, Schutz E.** 2013. Digital droplet PCR for rapid quantification of donor DNA in the circulation of transplant recipients as a potential universal biomarker of graft injury. Clin Chem **59:**1732–1741. http://dx.doi.org/10.1373/clinchem.2013.210328.
23. **Pholwat S, Stroup S, Foongladda S, Houpt E.** 2013. Digital PCR to detect and quantify heteroresistance in drug-resistant *Mycobacterium tuberculosis*. PLoS One **8:**e57238. http://dx.doi.org/10.1371/journal.pone.0057238.
24. **Taylor SC, Carbonneau J, Shelton DN, Boivin G.** 2015. Optimization of droplet digital PCR from RNA and DNA extracts with direct comparison to RT-qPCR: clinical implications for quantification of oseltamivir-resistant subpopulations. J Virol Methods **224:**58–66. http://dx.doi.org/10.1016/j.jviromet.2015.08.014.
25. **Bao Y, Bolotov P, Dernovoy D, Kiryutin B, Zaslavsky L, Tatusova T, Ostell J, Lipman D.** 2008. The influenza virus resource at the National Center for Biotechnology Information. J Virol **82:**596–601. http://dx.doi.org/10.1128/JVI.02005-07.
26. **Thompson JD, Gibson TJ, Plewniak F, Jeanmougin F, Higgins DG.** 1997. The CLUSTAL_X windows interface: flexible strategies for multiple sequence alignment aided by quality analysis tools. Nucleic Acids Res **25:**4876–4882. http://dx.doi.org/10.1093/nar/25.24.4876.
27. **Huggett JF, Foy CA, Benes V, Emslie K, Garson JA, Haynes R, Hellemans J, Kubista M, Mueller RD, Nolan T, Pfaffl MW, Shipley GL, Vandesompele J, Wittwer CT, Bustin SA.** 2013. The digital MIQE guidelines: minimum information for publication of quantitative digital PCR experiments. Clin Chem **59:**892–902. http://dx.doi.org/10.1373/clinchem.2013.206375.
28. **Devonshire AS, Honeyborne I, Gutteridge A, Whale AS, Nixon G, Wilson P, Jones G, McHugh TD, Foy CA, Huggett JF.** 2015. Highly reproducible absolute quantification of *Mycobacterium tuberculosis* complex by digital PCR. Anal Chem **87:**3706–3713. http://dx.doi.org/10.1021/ac5041617.
29. **Bustin SA, Benes V, Garson JA, Hellemans J, Huggett J, Kubista M, Mueller R, Nolan T, Pfaffl MW, Shipley GL, Vandesompele J, Wittwer CT.** 2009. The MIQE guidelines: minimum information for publication of quantitative real-time PCR experiments. Clin Chem **55:**611–622. http://dx.doi.org/10.1373/clinchem.2008.112797.
30. **Carr MJ, Gunson R, Maclean A, Coughlan S, Fitzgerald M, Scully M, O'Herlihy B, Ryan J, O'Flanagan D, Connell J, Carman WF, Hall WW.** 2009. Development of a real-time RT-PCR for the detection of swine-lineage influenza A (H1N1) virus infections. J Clin Virol **45:**196–199. http://dx.doi.org/10.1016/j.jcv.2009.06.001.
31. **Dube S, Qin J, Ramakrishnan R.** 2008. Mathematical analysis of copy number variation in a DNA sample using digital PCR on a nanofluidic device. PLoS One **3:**e2876. http://dx.doi.org/10.1371/journal.pone.0002876.
32. **Whale AS, Cowen S, Foy CA, Huggett JF.** 2013. Methods for applying accurate digital PCR analysis on low copy DNA samples. PLoS One **8:**e58177. http://dx.doi.org/10.1371/journal.pone.0058177.
33. **Ellison SLR, Barwick VJ, Farrant TJD.** 2009. Practical statistics for the analytical scientist: a bench guide, 2nd ed. The Royal Society of Chemistry, Cambridge, United Kingdom.
34. **Abramowitz M, Stegun IA.** 1972. Handbook of mathematical functions with formulas, graphs, and mathematical tables, 9th ed. Dover, New York, NY.
35. **Ngaosuwankul N, Noisumdaeng P, Komolsiri P, Pooruk P, Chokephaibulkit K, Chotpitayasunondh T, Sangsajja C, Chuchottaworn C, Farrar J, Puthavathana P.** 2010. Influenza A viral loads in respiratory samples collected from patients infected with pandemic H1N1, seasonal H1N1 and H3N2 viruses. Virol J **7:**75. http://dx.doi.org/10.1186/1743-422X-7-75.
36. **Grant PR, Kidd IM.** 2011. Rapid real-time PCR for detection of oseltamivir resistant pandemic influenza, abstr P33. Abstr Winter Meet Eur Soc Clin Virol. European Society for Clinical Virology, London, United Kingdom.
37. **Huggett JF, Cowen S, Foy CA.** 2015. Considerations for digital PCR as an accurate molecular diagnostic tool. Clin Chem **61:**79–88. http://dx.doi.org/10.1373/clinchem.2014.221366.
38. **Rome C, Esposito C, Rachiglio AM, Pasquale R, Iannaccone A, Chicchinelli N, Franco R, Mancini R, Pisconti S, De Luca A, Botti G, Morabito A, Normanno N.** 2013. Detection of EGFR mutations by TaqMan mutation detection assays powered by competitive allele-specific TaqMan PCR technology. Biomed Res Int **2013:**385087. http://dx.doi.org/10.1155/2013/385087.
39. **Kiselinova M, Pasternak AO, De Spiegelaere W, Vogelaers D, Berkhout B, Vandekerckhove L.** 2014. Comparison of droplet digital PCR and seminested real-time PCR for quantification of cell-associated HIV-1 RNA. PLoS One **9:**e85999. http://dx.doi.org/10.1371/journal.pone.0085999.
40. **White RA, III, Quake SR, Curr K.** 2012. Digital PCR provides absolute quantitation of viral load for an occult RNA virus. J Virol Methods **179:**45–50. http://dx.doi.org/10.1016/j.jviromet.2011.09.017.
41. **Hayden RT, Gu Z, Ingersoll J, Abdul-Ali D, Shi L, Pounds S, Caliendo AM.** 2013. Comparison of droplet digital PCR to real-time PCR for quantitative detection of cytomegalovirus. J Clin Microbiol **51:**540–546. http://dx.doi.org/10.1128/JCM.02620-12.
42. **Roberts CH, Last A, Molina-Gonzalez S, Cassama E, Butcher R, Nabicassa M, McCarthy E, Burr SE, Mabey DC, Bailey RL, Holland MJ.** 2013. Development and evaluation of a next-generation digital PCR diagnostic assay for ocular *Chlamydia trachomatis* infections. J Clin Microbiol **51:**2195–2203. http://dx.doi.org/10.1128/JCM.00622-13.
43. **Vanspauwen MJ, Wolffs PF, Franssen FM, Bruggeman CA, Wouters EF, Linssen CF.** 2014. Comparison of three different techniques for the isolation of viral RNA in sputum. J Clin Virol **61:**265–269. http://dx.doi.org/10.1016/j.jcv.2014.07.012.
44. **Falsey AR, Formica MA, Walsh EE.** 2012. Yield of sputum for viral detection by reverse transcriptase PCR in adults hospitalized with respiratory illness. J Clin Microbiol **50:**21–24. http://dx.doi.org/10.1128/JCM.05841-11.
45. **Nixon G, Garson JA, Grant P, Nastouli E, Foy CA, Huggett JF.** 2014. A comparative study of sensitivity, linearity and resistance to inhibition of digital and non-digital PCR and LAMP assays for quantification of human cytomegalovirus. Anal Chem **86:**4387–4394. http://dx.doi.org/10.1021/ac500208w.
46. **Huggett JF, Garson J, Whale AS.** Digital PCR and its potential application to microbiology. *In* Persing DH, Tenover FC, Hayden RT, Leven G, Miller MB, Nolte FS (ed), Molecular microbiology: diagnostic principles and practice, 3rd ed, in press. ASM Press, Washington, DC.
47. **Rittié L, Perbal B.** 2008. Enzymes used in molecular biology: a useful guide. J Cell Commun Signal **2:**25–45. http://dx.doi.org/10.1007/s12079-008-0026-2.
48. **Robasky K, Lewis NE, Church GM.** 2014. The role of replicates for error mitigation in next-generation sequencing. Nat Rev Genet **15:**56–62.
49. **Didelot A, Le Corre D, Luscan A, Cazes A, Pallier K, Emile JF,**

Laurent-Puig P, Blons H. 2012. Competitive allele specific TaqMan PCR for KRAS, BRAF and EGFR mutation detection in clinical formalin fixed paraffin embedded samples. Exp Mol Pathol **92:**275–280. http://dx.doi.org/10.1016/j.yexmp.2012.03.001.

50. **Worwa G, Andrade CC, Thiemann TC, Park B, Maharaj PD, Anishchenko M, Brault AC, Reisen WK.** 2014. Allele-specific qRT-PCR demonstrates superior detection of single nucleotide polymorphisms as genetic markers for West Nile virus compared to Luminex® and quantitative sequencing. J Virol Methods **195:**76–85. http://dx.doi.org/10.1016/j.jviromet.2013.09.014.
51. **Little S.** 2001. Amplification-refractory mutation system (ARMS) analysis of point mutations. Curr Protoc Hum Genet Chapter 9:Unit 9.8. http://dx.doi.org/10.1002/0471142905.hg0908s0.
52. **Morandi L, de Biase D, Visani M, Cesari V, De Maglio G, Pizzolitto S, Pession A, Tallini G.** 2012. Allele specific locked nucleic acid quantitative PCR (ASLNAqPCR): an accurate and cost-effective assay to diagnose and quantify KRAS and BRAF mutation. PLoS One **7:**e36084. http://dx.doi.org/10.1371/journal.pone.0036084.
53. **Ghedin E, Holmes EC, DePasse JV, Pinilla LT, Fitch A, Hamelin ME, Papenburg J, Boivin G.** 2012. Presence of oseltamivir-resistant pandemic A/H1N1 minor variants before drug therapy with subsequent selection and transmission. J Infect Dis **206:**1504–1511. http://dx.doi.org/10.1093/infdis/jis571.
54. **Pavsic J, Devonshire AS, Parkes H, Schimmel H, Foy CA, Karczmarczyk M, Gutierrez-Aguirre I, Honeyborne I, Huggett JF, McHugh TD, Milavec M, Zeichhardt H, Zel J.** 2015. Standardization of nucleic acid tests for clinical measurements of bacteria and viruses. J Clin Microbiol **53:**2008–2014. http://dx.doi.org/10.1128/JCM.02136-14.